Anodic growth of highly ordered titanium oxide nanotube arrays: Effects of critical anodization factors on their photocatalytic activity

Chin-Jung Lin [a], Yi-Hsien Yu [b], Szu-Ying Chen [b], and Ya-Hsuan Liou [b*]

Abstract—Highly ordered arrays of TiO_2 nanotubes (TiNTs) were grown vertically on Ti foil by electrochemical anodization. We controlled the lengths of these TiNTs from 2.4 to 26.8 μm while varying the water contents (1, 3, and 6 wt%) of the electrolyte in ethylene glycol in the presence of 0.5 wt% NH_4F with anodization for various applied voltages (20–80 V), periods (10–240 min) and temperatures (10–30 °C). For vertically aligned TiNT arrays, not only the increase in their tube lengths, but also their geometric (wall thickness and surface roughness) and crystalline structure lead to a significant influence on photocatalytic activity. The length optimization for methylene blue (MB) photodegradation was 18 μm. Further extending the TiNT length yielded lower photocatalytic activity presumably related to the limited MB diffusion and light-penetration depth into the TiNT arrays. The results indicated that a maximum MB photodegradation rate was obtained for the discrete anatase TiO_2 nanotubes with thick and rough walls.

Keywords—anodic oxidation, nanotube, photocatalytic, TiO_2

I. INTRODUCTION

PHOTOCATALYTIC degradation of harmful organic pollutants using nanoparticulate semiconductors has been extensively investigated for waste treatment [1−5].Owing to its inexpensive, non-toxic nature, large band gap, and chemical stability, titanium oxide (TiO_2) is the most applied semiconductor, for example, in the effective decomposition of dyes to benign by-products in textile effluent treatment [6, 7]. TiO_2 as photocatalyst present in aqueous systems has been applied in either immobilized or suspended forms. The former, that is, the immobilization of powdered TiO_2 as a film onto various substrates, has been recognized as being more preferable to the latter because this application can ignore particle aggregation and minimize post-treatment processes [8]. However, the photocatalytic activities of these TiO_2-nanoparticle films rely on the rapid recombination of photogenerated electron-hole pairs, limited mass transport of reactants/products and short light-penetration depth, hindering

its feasibility for extensive applications. It is expected that the arrangement of ordered one-dimensional (1-D) arrays (e.g., tubes, rods, and wires) perpendicular to substrates would suppress charge recombination, provide easy access to the surface, and permit light scattering within a 1-D structure, leading to high photocatalytic activity.

Electrochemical anodization of Ti metal is a relatively simple approach for fabricating vertically oriented TiO_2-nanotube (TiNT) arrays directly grown on the Ti substrate [9−12]. As initially reported by Zwilling et al. in 1999 [13], the first generation TiO_2 nanotube arrays had a limited length of a few hundred nanometers that grew during anodization of Ti foil in aqueous HF-based electrolyte. In the second generation, the TiNT lengths were increased to a few micrometers by adjusting the electrolyte pH [10]. Most recently, Grimes and co-workers [14] have described the fabrication of oriented TiO_2 nanotube arrays by anodic oxidation of Ti foil in non-aqueous organic electrolytes (e.g., ethylene glycol, formamide, and dimethyl sulfoxide) having tens to hundreds of micrometers in length. However, these photocatalytic applications are mostly influenced by surface area, as well as the geometric and crystalline structure of TiNT arrays that can be controlled by tailoring the anodization and growth medium variables.

In the present study, the anodic growth of oriented TiO_2 nanotubes on Ti-metal foil was conducted in ethylene glycol-based electrolyte. Photocatalytic performances of the resulting TiNT films were evaluated by bleaching methylene blue solution through UV irradiation. We investigated some critical anodization factors, including anodization time, applied potential, anodization temperature, and water content in the electrolyte, for the growth of the tubular structures that would significantly influence its photocatalytic activity.

II. EXPERIMENTAL SECTION

A. Fabrication of TiNT

Titanium foils with thickness of about 300 μm (>99.5% purity, Allegheny Ludlum) were firstly mechanically polished with different abrasive papers, and then ultrasonically degreased in acetone, methanol, and deionized water (DI) in turn, followed by rinsing with DI water and drying in a nitrogen

[a.] National Ilan University, 1, Sec. 1, Shen-Lung Road, I-Lan, 260, Taiwan.
[b.] Department of Geosciences, National Taiwan University, P.O. Box 13-318, Taipei 106, Taiwan.
*Corresponding author e-mail address: yhliou@ntu.edu.tw; Phone: +886-2-33662930; Fax: +886-2-23636095.

stream. The sample were anodized in ethylene glycol containing 0.5 wt.% NH_4F (Alfa Aesar, 96%) and different water content (1, 3, and 6 wt%) by using a two-electrode electrochemical cell with a platinum foil as a counter electrode. The applied voltages were controlled at 40, 60, and 80 V (provide by a DC power supply (GW Instek, GPR-30H10D) and the electrolyte temperatures were at 10, 20, and 30 ^{o}C (controlled by a double-walled cooling system). After anodization, the prepared TiNT/Ti was thoroughly washed with a large amount of DI water and methanol to remove precipitation atop titanium oxides and then dried by argon flow. The as-anodized TiNT arrays were amorphous; to induce crystallinity, they were subsequently annealed at 450 ^{o}C (heating rate of 5 $^{o}C/min$) for 3 h in oxygen gas (flow rate of 50 mL/min).

B. Sample Characterization

The morphologies and the thickness measurement of the prepared TiNT arrays were examined with field-emission scanning electron microscopy (FESEM, FEI, Quanta 200F). X-ray diffraction (XRD, Philips, X' Pert) patterns were carried out in a D/max-2500 powder diffractometer using Cu $K\alpha(\lambda=1.54$ Å) radiation.

An estimate of the surface roughness can be deduced from $(Bu_4N)_2Ru(dcbpyH)_2(NCS)_2$ (N-719 dye, Solaronix) adsorption measurements. The TiNT arrays were immersed in 0.3 mM N-719/ethanol for 24 h and then rinsed using acetonitrile, followed by dissolving absorbed N-719 completely from the TiNT arrays to a 0.2 M sodium hydroxide solution. The concentrations of N-719 dye were determined by UV-Vis spectroscopy (U-3410, Hitachi). The N-719 dye molecule in the TiNT arrays was expected for monolayer coverage of the inside and outside of the tubes and a dye molecule footprint of 1.6 nm^2 [15] was used.

C. Photodegradation Experiments

Methylene blue (MB), a representative of organic dyes in textile effluents, was considered as a model contaminant in the purification of dye waste water. The prepared TiNT samples, cut into the same size of 0.5 cm × 1.0 cm, were vertically placed in 3 mL rectangular quartz reactor containing 10 mg/L MB solution. The photoirradiation employed a wavelength of 300 nm light as UV light source, and the relative concentration of MB in the solution is determined through UV-Vis spectroscopy (HITACHI, U-3900) by comparing its intensity of the 662 nm absorption with that of the initial MB solution. The sample was immersed in the MB solution to stay in the dark for 30 min, and then the UV light was turned on. All experiments were duplicated or triplicated. Direct photolysis as a control experiment shows that in the absence of TiO_2 photocatalyst decoloration of the dye solution reached near 10%, indicating the photostability of MB under UV light within the irradiation period of 4 h.

III. RESULTS AND DISCUSSION

Highly ordered TiNT arrays with various tube lengths from 2.4 to 26.8 μm were prepared using anodic oxidation of Ti foil

at 80 V in ethylene glycol solution containing 3 wt% H_2O and 0.5 wt % NH_4F at 20 °C at the anodization time of 10 to 240 min. Fig. 1a–1d exhibit the typical morphology of the 12.8 μm long TiNT arrays, examined by FESEM. The top surface shows that there is a fully developed nanotube array with inner diameter of approximatly 100 nm and a wall thickness of 15 nm (Fig. 1 a). The regular and well-aligned TiNT arrays with rough walls were observed in Fig. 1 b where regulary spaced rings formed on the side wall. The ring spacing, specially depending on the electrochemical condition [10], would strongly influence the surface roughness of the nanotubes related to photon-absorption efficiency. The pore mouths are open on the top of the layer, while the bottom of the tube are closed (Fig. 2 c). The film thickness was 12.8 μm, which was directly measured through the SEM cross-sectional image of the intentional bent sample (Fig. 1 d).

Photodegradation of MB under 300 nm irradiation was performed to investigate the photocatalytic activities of the
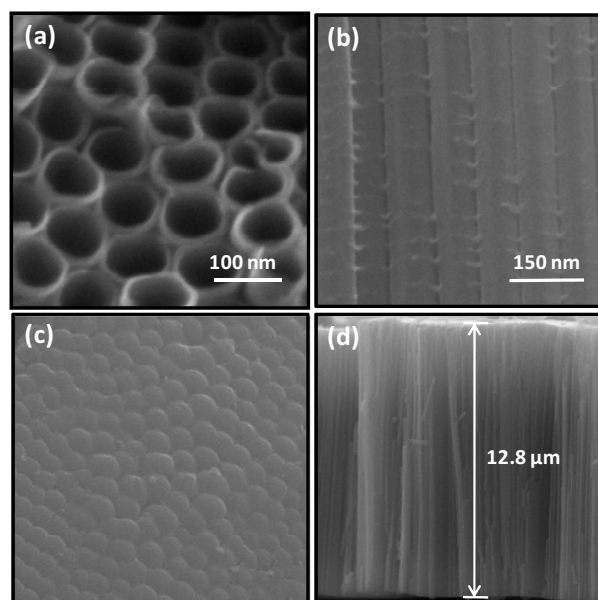

Fig. 1 SEM images of TiNT obtained by anodization of 80 V at 20 ^{o}C in 0.5 wt% NH_4F/ethylene glycol with water addition of 3 wt% for 60 min. (a) top view; (b) side view; (c) bottom view; (d) film thickness.
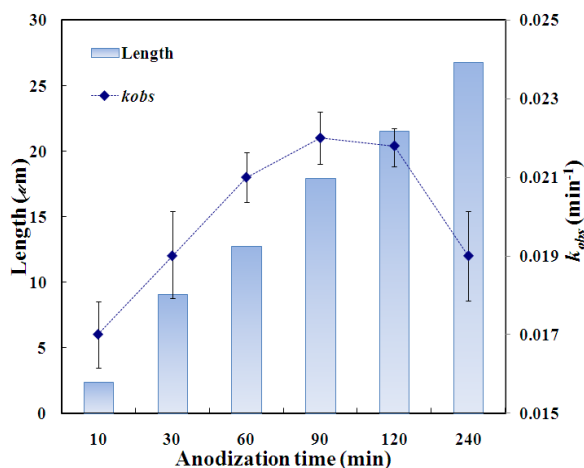
Fig. 2 Dependence of photocatalytic activity of TiNT length by anodization of 80 V at 20 °C in 0.5 wt% NH_4F/ethylene glycol with water addition of 3 wt% for various anodization periods.

prepared TiNT arrays. A first-order rate model, Eq. (1), effectively describes the photocatalytic decoloration of the MB solution that has also been observed previously [16].

$$-dC/dt = k_{obs} \times C \qquad (1)$$

where C refers to the concentration of methylene blue, t is the reaction time (min), and k_{obs} is the observed rate constant (min^{-1}). Fig. 2 shows the values of several TiNT arrays prepared with different tube lengths controlled by anodization times. As shown in Fig. 2, the length of TiNT arrays linearly increases with the increase in anodization time (about 2.4 μm at 10 min to 26.8 μm after 240 min). However, the photocatalytic degradation of MB using TiNT arrays does not follow the same trend. The value of k_{obs} increases continuously with the TiNT length, and declines above an upper limit with 18 μm length. Accordingly, the length optimization for the photocatalytic activity is 18 μm, as indicated in Fig. 2. Further extending the TiNT length yields lower photocatalytic activity possibly related to the limited MB diffusion and light-penetration depth into the TiNT arrays.

The equilibrium between the electrochemical formation of TiO_2 (2) and chemical dissolution of TiO_2 by the presence of fluoride-containing electrolyte (3) is the determining factor in the nanotube self-assembly [11, 17].

$$Ti + 2H_2O \rightarrow TiO_2 + 4H^+ \qquad (2)$$

$$TiO_2 + 6HF \rightarrow [TiF_6]^{2-} + 2H_2O + 2H^+ \qquad (3)$$
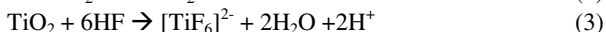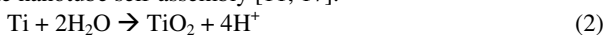
The formation rate of TiO_2 at the metal-oxide interface is highly dependent on the etching rate of titanium (Ti^0 is oxidized to Ti^{4+} and then migrates outwards) and the availability of O^{2-} donor (O^{2-} ions migrate towards the metal-oxide interface) in the electrolyte. The chemical dissolution rate of TiO_2 is strongly controlled by the field-assisted migration of electrolyte anions, especially F^- which competes with O^{2-} migration [18]. However, the nanotubes cannot be formed if the chemical dissolution is too high or too low, which results in either rapid or very slow oxide
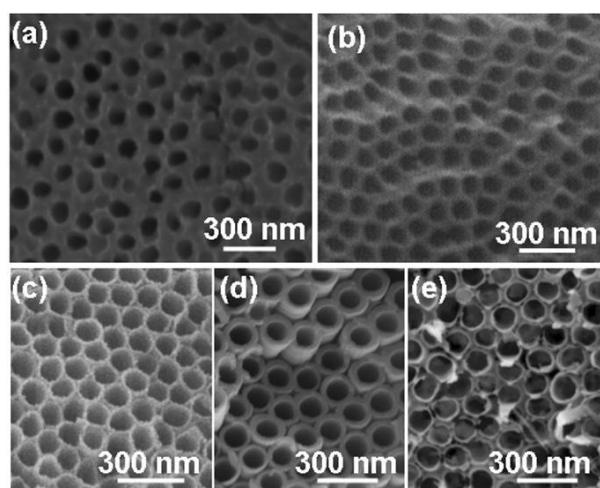

Fig. 3 Top-view SEM images of TiNT arrays obtained at 20 °C with (a) 40 V, (b) 60 V, and (c) 80 V for 30 min in the electrolyte containing 0.5 wt% NH_4F and 3 wt% H_2O. At the same conditions with the constant voltage of 80 V, the top-view SEM images of TiNT obtained at (d) 10 °C and (e) 30 °C.

formation. For example, the rapid dissolution of TiO_2 in aqueous electrolyte containing HF resulted in the TiNT thickness in the range of hundreds of nanometer [19]. With anhydrous organic electrolytes, the donation of oxygen is more difficult than that of water, thus the reduced tendency for stable TiO_2 formation leads to a compact thick oxide layer with irregular features. We controlled applied potential, anodization temperature, and water content in the electrolyte for the growth of the tubular structures and investigated their influence on the photocatalytic activity.

A. Effect of the Anodization Potential

Scanning electron microscope (SEM) micrographs in Fig. 3a-c show the significant difference in top surface morphologies of the TiNT arrays prepared with various applied potentials (40 V, 60 V, and 80 V) in the ethylene glycol containing 0.5 wt% NH_4F and 3 wt% H_2O at 20 °C. For higher potentials (e.g. 100 V), sparking at the interface of Ti foil and electric-conduction Cu wire was observed and the electrolyte temperature was not readily controlled as that in low potential. Thus, it is not feasible to extend the applied potential above 80 V in the electrochemical anodization. At 40 V, it is observed that ordered porous networks occurred. With the applied potential increases, a nanoporous structure (Fig. 3a) transforms to a discrete tubular appearance (Fig. 3c). However, an increase in the formation potential does not strongly affect the diameter at the pore mouth. It remains about 100 nm, independent for applied potentials. As indicated in Table 1, the lengths of the TiNT arrays prepared with 40, 60, and 80 V are 4.5, 8.7, and 8.8 μm, respectively, and their surface roughnesses are 5.2, 10.4, and 13.1 $μm^{-1}$, respectively. The growth of tubular structure slows down at the potential of 40V whereas the

Table 1

Dependence of photocatalytic activity of TiNT by anodization at 20 °C in 0.5 wt% NH$_4$F/ethylene glycol with water addition of 3 wt% for various anodization potential.

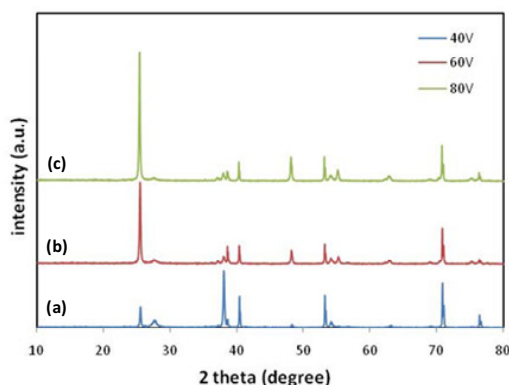| Potential (V)	TiNT Length (μm)	Surface roughness (μm^{-1})	k$_{obs}$ (10^{-3} min^{-1})
80 V	8.8	13.1	19.3 ± 0.9
60 V	8.7	10.4	16.7 ± 1.0
40 V	4.5	5.2	8.1 ± 0.7

Fig. 4 XRD pattern of the TiNT arrays obtained at 20 °C with (a) 40 V, (b) 60 V, and (c) 80 V for 30 min in the electrolyte containing 0.5 wt% NH$_4$F and 3 wt% H$_2$O.

well-ordered TiO$_2$ nanotube arrays can be fully developed in the aqueous electrolyte containing HF at the potential above 10 V [19]. The difference in the polarity between ethylene glycol and water might cause fluoride ions not easily migrate to the oxide interface in ethylene glycol [20], thus high field-assisted migration of fluoride ions for the chemical dissolution of TiO$_2$ would be needed to form tubular structure.

Fig. 4 presents the x-ray diffration patterns of the TiNT arrays obtained with different applied potentials from 40 to 80 V after being annealed at 450 °C for 3 h in oxygen gas. As shown, the diffraction peaks at 2θ of 25.3°, 37.1°, 37.9°, 48.1°, 54.0°, and 55.2° can be indexed to the characteritic peaks of anatase phase (JCPDS No 89-4921). The other peaks are the characteristic peaks of the original Ti foil. All of these anatase-phase peaks are enhanced by the increased length of the TiNT arrays. As the applied potential decreased, rutile peak at 2θ of 27.5° also began to appear and resulted in the progressive decrease of anatase/rutile ratios.

Photocatalytic performances of the TiNT arrays obtained with the applied potentials of 40, 60, and 80 V were evaluated via bleaching MB solution by UV irradiation. The resulting values of k$_{obs}$ (see Table 1) are (8.1 ± 0.7) ×10^{-3} min^{-1}, (16.7 ± 1.0) ×10^{-3} min^{-1}, and (19.3 ± 0.9) ×10^{-3} min^{-1} for the TiNT arrays prepared at 40, 60, and 80 V, respectively. The low photocatalytic activity of the TiNT arrays prepared at 40 V might be ascribed to (i) the incomplete tubular structure with

Table 2
Dependence of photocatalytic activity of TiNT by anodization

potential of 80 V in 0.5 wt% NH$_4$F/ethylene glycol with water addition of 3 wt% for various anodization temperature.

Temperature (°C)	TiNT Length (μm)	Wall thickness (nm)	Inner pore diameter (nm)	Surface roughness (μm^{-1})	k$_{obs}$ (10^{-3} min^{-1})
10°C	8.4	35	99	12.6	22.3 ± 0.8
20°C	8.8	15	102	13.1	19.3 ± 0.9
30°C	8.9	10	105	13.8	13.2 ± 0.6

short thickness and smooth surface that allowed less effective photons for photocatalysis, and (ii) the presence of rutile phase that is much worse than anatase phase in photocatalytic activity. The 15% difference in the photocatalytic activity between the TiNT arrays prepared at 60 V and 80 V with the similar length implies the tube with rough wall absorbs more photons for MB photodegradation.

B. Effect of the Electrolyte Temperature

The TiNT arrays were anodized at 80 V at three different electrolyte temperatures: 10 °C, 20 °C, and 30 °C. The top-view SEM micrographs of the TiNT arrays prepared at 10 °C, 20 °C, and 30 °C, shown in Fig. 3c-3e, reveal that only geometric parameter that changes significantly is the wall thickness. The values listed in Table 2 are 35, 15, and 10 nm for the TiNT arrays prepared at 10 °C, 20 °C, and 30 °C, respectively. The wall thickness increases with decreasing electrolyte temperature. Tube length, surface roughness, and pore diameter are relative constant in these three samples. The nanotube walls are thicker in the TiNT arrays prepared at 10 °C than those prepared at 20 °C and 30 °C, indicating that this film contains a larger amount of TiO$_2$ per unit length. It was observed that some rupture occurs near the tube top prepared at 30 °C. During anodization, the fluoride ions move to the tip of the tube at the TiO$_2$/Ti interface under a high electrical filed, leading to a decay of the F$^-$ concentration towards to the tube top. Their accumulation results in a fluoride-rich area at the tube bottom to constantly chemical dissolve TiO$_2$ for tube growth, independent of the electrolyte temperature. Instead, chemical dissolution of the TiO$_2$ wall at the tube top by small fluoride ions slows down due to the low electrolyte temperature. Accordingly, the electrolyte temperature significant influences the wall thickness at the tube top, but has a negligible effect on the tube growth. Table 2 indicates the resulting values of k$_{obs}$ are (22.3 ± 0.8) ×10^{-3} min^{-1}, (19.3 ± 0.9) ×10^{-3} min^{-1}, and (13.2 ± 0.6) ×10^{-3} min^{-1} for the TiNT arrays prepared at 10 °C, 20 °C, and 30 °C, respectively. The photocatalytic degradation rate of MB by the TiNT arrays prepared at 10 °C is twice as much as that obtained by the TiNT arrays prepared at 30 °C. In agreement to the study reported by Mor et al. [11], the thicker tube walls provide enhanced band bending to decrease surface recombination rate of separated electrons and holes.

C. Effect of the Water Content in the Electrolyte

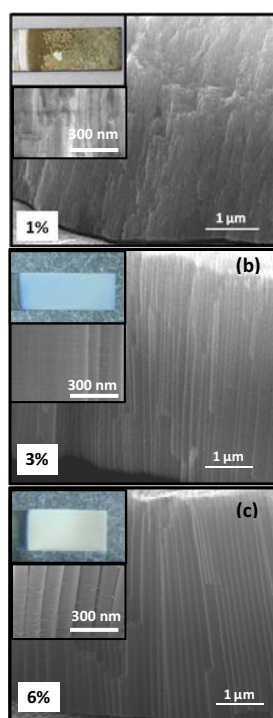Fig. 5a-c show the morphologies of the TiNT arrays with

Fig. 5 SEM images of the TiNT arrays obtained at 20 °C with 80 V for 30 min in the electrolyte containing 0.5 wt% NH$_4$F and water contain of (a) 1%, (b) 3%, (c)6%. The inset show specimen picture of the corresponding TiNT film.

similar length prepared by anodization of 80 V at 20 °C in 0.5 wt% NH$_4$F/ethylene glycol with water addition of 1 wt%, 3wt%, and 6wt%, respectively. The growth rate of TiNT decreased with the increase in water content. The anodization times of 20, 30, and 80 min are necessary to grow ~8 μm-long TiNT arrays at 1 wt%, 3wt%, and 6wt% of water contents, respectively. For higher water content (e.g. 10 wt%), the current decreased rapidly to near zero in the initial stage of anodization. It took several hours to grow the TiNT to ~8 μm-long, thus anodization at higher water content is not applicable. As shown in Fig. 5a, the TiO$_2$ layer exhibits a sponge-like structure. After annealed, however, the rupturing and peeling of the TiNT readily occur (the inset of Fig. 5a). The resulting TiNT arrays were mechanically unstable, with a strong tendency towards crack development under the influence of even weak mechanical forces. These inevitably influence the mechanical stability and the photocatalytic activity. When the water content was more than 1 wt%, there was no significant change in the morphology of the nanotubes (Fig. 5b and 5c). However, the nanotubes formed in the water content of 6 wt% showed ridges on the tube wall and the number of the ridges increased with increase in water content (the insets of Fig. 5b and 5c). The surface roughnesses are 9.6, 13.1 and 14.8 μm^{-1} for the TiNT formed at the water content of 1 wt%, 3wt%, and 6wt%, respectively.
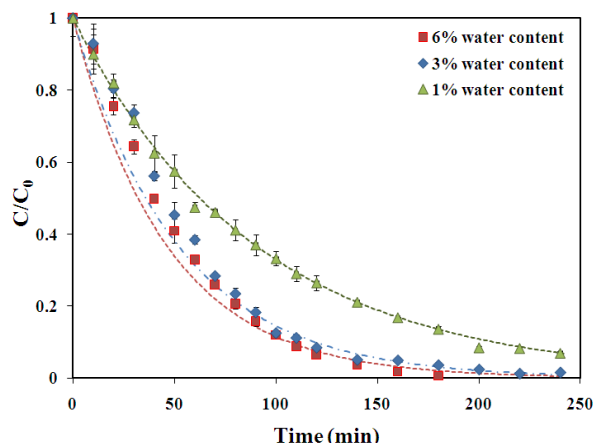

Fig. 6 Photodegradation kinetics of MB using the TiNT arrays obtained at 20 °C with 80 V for 30 min in the electrolyte containing 0.5 wt% NH$_4$F and various water contains.

Fig. 6 shows the C/Co versus time curves of the MB photodegradation using the TiNT arrays formed in the water content of 1 wt%, 3 wt%, and 6 wt%. All curves shown in Fig. 6 are fit well to the first-order reaction kinetic model. The k_{obs} values calculated from the slope of ln(C/C_o) versus time curves are $(11.1 \pm 0.4) \times 10^{-3}$ min^{-1}, $(19.3 \pm 0.9) \times 10^{-3}$ min^{-1}, and $(21.6 \pm 1.0) \times 10^{-3}$ min^{-1} for the TiNT arrays formed in the water content of 1 wt%, 3 wt%, and 6 wt%, respectively. The difference in the photocatalytic activity between the TiNT arrays prepared in the water content of 3 wt%, and 6 wt% with the similar length implies the tube with rough wall absorbs more photons to generate the photo-excited electrons reacting with MB in the solution. The rates of MB photodegradation using the two tubular structures are almost twice that using the sponge-like structure. The significant enhancement of the k_{obs} values obviously is not only attributed to the increase in surface roughness for absorbs more photons for MB photodegradation. Since the incident light is well directed within the tubes which are perpendicular to the Ti substrate, the light-penetration depth and the concentration of photogenerated electron-hole pairs can be increased for efficient MB photodegradation. By preparation parameters optimization for photocatalytic activity, we were able to further improve the MB photodegradation rate. The optimal k_{obs} value of $(28.6 \pm 1.2) \times 10^{-3}$ min^{-1} was achieved using the 18 μm-long TiNT arrays prepared by anodization of 80 V at 10 °C in the 0.5 wt% NH$_4$F/ethylene glycol with water addition of 6 wt%.

IV. CONCLUSIONS

In this work, highly ordered TiO$_2$-nanotube arrays with length of a few tens of micrometer and rough tube wall were fabricated using electrochemical anodization of Ti foil for methylene blue photodegradation. We controlled critical anodization factors, including anodization time, applied potential, anodization temperature, and water content in the electrolyte, for the growth of the tubular structures. Substantial

improvement on the photocatalytic activity has been demonstrated when the prepared TiNT arrays have about 18 μm in length, as well as discrete anatase TiO_2 nanotubes with thick and rough walls. Because of the facile preparation of anodic-oriented TiO_2-nanotube arrays, as well as their well-controllable morphology, and easy access to photons and reactants, the application of such arrays is expected to facilitate the development of photocatalytic technique for environmental purification.

REFERENCES

[1] Mills, A., Davies, R. H., and Worsley, D., "Water purification by semiconductor photocatalysis," *Chem. Soc. Rev.,* vol. 22, pp. 417-425, 1993.

[2] Asahi, R., Morikawa, T., Ohwaki, T., Aoki, K. and Taga, Y., "Visible-light photocatalysis in nitrogen-doped titanium oxides," *Science.,* vol. 293, pp. 269-271, 2001.

[3] Li, X. Z. and Li, F. B., "Study of Au/Au^{3+}-TiO$_2$ photocatalysts toward visible photooxidation for water and wastewater treatment," *Environ. Sci. Technol.*, vol. 35, pp. 2381-2387, 2001.

[4] Lee, J. C., Kim, M. S., and Kim, B. W., "Removal of paraquat dissolved in a photoreactor with TiO$_2$ immobilized on the glass-tubes of UV lamps," *Water Res.*, vol. 36, pp. 1776-1782, 2002.

[5] Zhang, X., Pan, J. H., Du, A. J., Fu, W., Sun, D. D., Leckie, J. O., "Combination of one-dimensional TiO$_2$ nanowire photocatalytic oxidation with microfiltration for water treatment," *Water Res.*, vol. 43, pp. 1179-1186, 2009.

[6] Kar, A., Smith, Y. R., and Subramanian, V., "Improved photocatalytic degradation of textile dye using titanium dioxide nanotubes formed over titanium wires. Environ," *Sci. Technol.*, vol. 43 (9), pp. 3260-3265, 2009.

[7] Kumar, P. S. S., Sivakumar, R., Anandan, S., Madhavan, J., Maruthamuthu, P., and Ashokkumar, M., "Photocatalytic degradation of Acid Red 88 using Au–TiO$_2$ nanoparticles in aqueous solutions," *Water Res.*, vol. 42, pp. 4878-4884, 2008.

[8] Wu, J. J. and Tseng, C. H., "Photocatalytic properties of nc-Au/ZnO nanorod composites," *Appl. Catal. B: Environ.*, vol. 66, pp. 51-57, 2006.

[9] Gong, D., Grimes, C. A., Varghese, O. K., Hu, W., Singh, R. S., Chen, Z., and Dickey, E. C., "Titanium oxide nanotube arrays prepared by anodic oxidation," *J. Mater. Res.*, vol. 16 (12), pp. 3331-3334, 2001.

[10] Tsuchiya, H., Macak, J. M., Ghicov, A., Taveira, L., Balaur, E., Ghicov, A., Sirotna, L., and Schumuki, P., "Self-organized TiO$_2$ nanotubes prepared in ammonium floride containing acetic acid electrolytes," *Electrochem. Commun.*, vol. 7, pp. 576-580, 2005.

[11] Mor, G. K., Shankar, K., Paulose, M., Varghese, O. K., and Grimes, C. A., "Enhanced photocleavage of water using titania nanotube arrays," *Nano Lett.*, vol. 5, pp. 191-195, 2005.

[12] Zheng, Q., Zhou, B., Bai, J., Li, L., Jin, Z., Zhang, J., Li, J., Liu, Y., Cai, W., and Zhu, X., "Self-organized TiO$_2$ nanotube array sensor for the determination of chemical oxygen demand," *Adv. Mater.*, vol. 20, pp. 1044-1049, 2008.

[13] Zwilling, V., Aucouturier, M., and Darque-Ceretti, E., "Anodic oxidation of titanium and TA6V alloy in chromic media. An electrochemical approach," *Electrochim. Acta.*, vol. 45, pp. 921-929, 1999.

[14] Shankar, K., Mor, G. K., Fitzgerald, A., and Grimes, C. A., "Cation effect on the electrochemical formation of very high aspect ratio TiO$_2$ nanotube arrays in formamide-water mixtures," *J. Phys. Chem. C.*, vol. 111, pp. 21-26, 2007.

[15] Grätzel, M., "Molecular photovoltaics that mimic photosynthesis," *Pure Appl. Chem.*, vol. 73 (3), pp. 459-467, 2001.

[16] Guettai, N. and Ait Amar, H., "Photocatalytic oxidation of methyl orange in presence of titanium dioxide in aqueous suspension. Part II: kinetics study," *Desalination,* vol. 185, pp. 439-448, 2005.

[17] Chanmanee, W., Watcharenwong, A., Chenthanmarakshan, C. R., Kajitvichyanukul, P., de Tacconi, N. R., and Rajeshwar, K., "Formation and characterization of self-organized TiO$_2$ nanotube arrays by pluse anodization," *J. Am. Chem. Soc.*, vol. 130, pp. 965-974, 2008.

[18] Habazaki, H., Fushimi, K., Shimizu, K., Skeldon, P., and Thompson, G. E., "Fast migration of fluoride ions in growing anodic titanium oxide," *Electrochem. Commun.*, vol. 9, pp. 1222-1227, 2007.

[19] Mor, G. K., Varghese, O. K., Paulose, M., Shankar, K., and Grimes, C. A., "A review on highly ordered, vertically oriented TiO$_2$ nanotube arrays: Fabrication, material properties, and solar energy applications," *Solar Energy Materials and Solar Cells*, vol. 90, pp. 2011-2075, 2006.

[20] Christophersen, M., Carstensen, J., Voigt, K., and Föll, H., "Organic and aqueous electrolytes used for etching macro- and mesoporous silicon," *Phys. Stat. sol. (a)*, vol. 197 (1), pp. 34-38, 2003.